Nanoscale

Accepted Manuscript

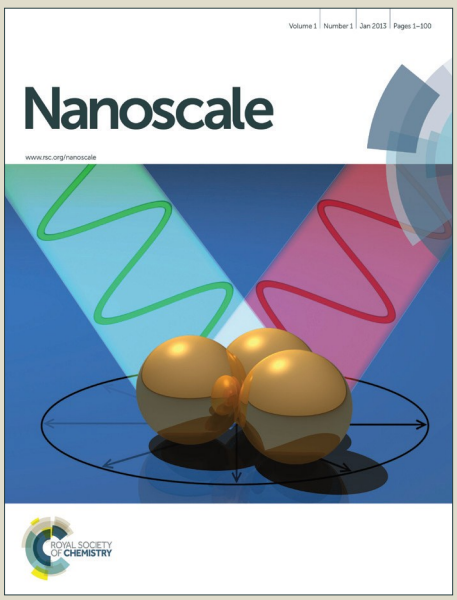

This is an *Accepted Manuscript*, which has been through the Royal Society of Chemistry peer review process and has been accepted for publication.

Accepted Manuscripts are published online shortly after acceptance, before technical editing, formatting and proof reading. Using this free service, authors can make their results available to the community, in citable form, before we publish the edited article. We will replace this *Accepted Manuscript* with the edited and formatted *Advance Article* as soon as it is available.

You can find more information about *Accepted Manuscripts* in the Information for Authors.

Please note that technical editing may introduce minor changes to the text and/or graphics, which may alter content. The journal's standard Terms & Conditions and the Ethical guidelines still apply. In no event shall the Royal Society of Chemistry be held responsible for any errors or omissions in this *Accepted Manuscript* or any consequences arising from the use of any information it contains.

ROYAL SOCIETY OF CHEMISTRY

www.rsc.org/nanoscale

A silicon nanocrystals/polymer nanocomposite as down-conversion layer in organic and hybrid solar cells

V. Svrcek[1], T. Yamanari[1], D. Mariotti[2], S. Mitra[2], T. Velusamy[2], K. Matsubara[1]

[1]Research Center for Photovoltaic Technologies, National Institute of Advanced Industrial Science and Technology (AIST), Central 2, Umezono 1-1-1, Tsukuba, 305-8568, Japan

[2]Nanotechnology & Integrated Bio-Engineering Centre (NIBEC), University of Ulster, UK

Abstract: Silicon nanocrystals (Si-ncs) down-conversion is demonstrated to enhance organic and hybrid organic/inorganic bulk heterojunction solar cells based on PTB7:[70]PCBM bulk heterojunction devices. Surfactant free surface-engineered Si-ncs can be integrated in the device architecture to be optically active and provide a mean of effective down-conversion for blue photons (high energy photons below ~450 nm) into red photons (above ~680 nm) leading to 24% enhancement of the photocurrent under concentrated sunlight. We also demonstrate that the down-conversion effect under 1-sun is enhanced in the case of hybrid solar cells where engineered Si-ncs are also included in the active layer.

Keyword: hybrid photovoltaic; silicon nanocrystal; surface engineering; concentrator sunlight.

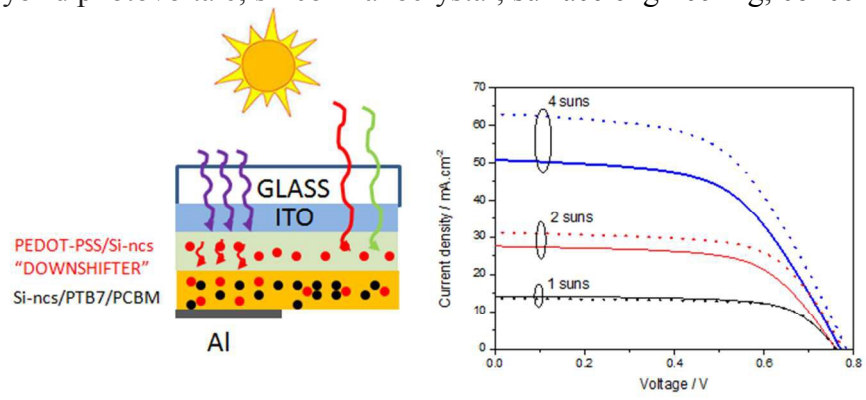

TOC figure

Nanoscale Accepted Manuscript

1. Introduction

Colloidal semiconducting nanocrystals with quantum confinement, also known as quantum dots, represent an example of advanced nanotechnology with potential impact on a range of optoelectronic applications including light emitting diodes and photovoltaic devices [1-7]. Si-ncs exhibit unique physical phenomena that could contribute to substantial enhancement in the conversion efficiency of next generation PV devices [4, 7]; when Si-ncs are integrated in the active/absorbing layer, strong electronic coupling between neighboring Si-ncs can lead to the formation of collective states, mini-bands, and/or to carrier multiplication [4]. Alternatively, Si-ncs can be used for down-conversion when integrated in the front end of solar cells [8]. This could be particularly beneficial for polymer solar cells since the degradation of organic devices is largely attributed to the polymer absorption of ultraviolet (UV) photons through photobleaching photooxidation [9]. Therefore, the use of highly photoluminescent and surface-engineered Si-ncs represents an attractive option for the management of UV-photons and high photon fluxes through three different but closely linked mechanisms [10]. Firstly, Si-ncs absorption in the UV region prevents high energy photons reaching the polymeric active layer reducing UV-induced degradation; secondly, undesired high-energy photons are converted into useful lower energy ones via room temperature PL [11, 12]. Thirdly, the PL of Si-ncs is expected to be enhanced under high intensity radiation [10] so that the blue-to-red photon conversion becomes even more efficient under high photon fluxes or concentrated light. It is clear that organic devices are not suitable for technologies based on highly concentrated light and are not expected to compete with III-V layers which typically use 300-500 suns [13]. Nevertheless there is substantial interest in improving the performance of organic devices under high intensity light that is due to varying weather and geographical conditions (> 1 sun) [14]. Furthermore, preventing degradation by UV

Nanoscale Accepted Manuscript

radiation could also allow organic solar cells to become viable for low-concentration schemes (< 10-suns) that utilize low-cost concentrators [15, 16].

A crucial aspect for Si-ncs integration in PV devices is represented by the control of the surface characteristics [17]; quantum confinement effects are observed for small nanocrystal sizes (<10 nm in diameter) and at these dimensions the Si-ncs surface chemistry play a critical role for the overall optoelectronic properties and device performance. While the use of bulky and/or long molecular passivation is frequently used and it is effective in stabilizing the Si-ncs properties in colloids, it is highly detrimental for transport and device-related properties. For example, exciton dissociation and carrier transport suffer from the separation between Si-ncs due to the bulky surfactants. Recently, plasma-based approaches have been successfully applied to induce non-equilibrium chemical reactions on the surface of Si-ncs directly in colloids and to achieve surface-engineered Si-ncs without any bulky surfactants [18]. Such approaches led to the enhancement of the Si-ncs photoluminescence (PL) properties and their electronic interaction with polymer matrix [19] as well as Si-ncs long-term stability in liquids (including water [20]).

In this manuscript we report on the optical and opto-electronic contribution of surface-engineered Si-ncs in organic and hybrid solar cell devices. We demonstrate that a water-soluble hybrid nanocomposite formed by surface-engineered Si-ncs embedded in poly(3,4-ethylenedioxythiophene):poly(styrenesulfonate) (PEDOT:PSS) can be used to enhance the efficiency of organic and hybrid PV devices increasing the photocurrent.

Nanoscale Accepted Manuscript

2. Experimental details

Fabrication of the nanocomposite - Si-ncs with quantum confinement effects were produced by electrochemical etching of a silicon wafer and subsequent mechanical pulverization [18]. We have studied the properties and performed materials characterization of the Si-ncs produced by this method for a number of years [17,18] and our results are also in good agreement with the extensive literature on porous silicon (e.g. [21-23] and see also Supporting Information in [15]; additional details on the average size and size distribution can also be found in the Supporting Material).

The as-prepared Si-ncs powder (2.5 mg) was then dispersed in 5 mL ethanol. In order to induce surface chemical reactions without using surfactants, a radio-frequency (RF) microplasma at atmospheric pressure has been used; this microplasma process induces chemical reactions directly into the Si-ncs/ethanol colloid contributing to surface engineering the Si-ncs [17, 18]. The RF microplasma was generated within a quartz capillary between two ring-electrodes where a third ring-electrode was used for plasma ignition via a high voltage pulse. Because the microplasma was generated close to the end of the quartz capillary, a small plasma jet (~mm) could be formed outside the capillary. Pure helium gas was flown inside the quartz capillary at the rate of 250 sccm. The 450 MHz applied power was kept at 60 W. The distance between the end of the quartz capillary and the surface of liquid dispersion was adjusted around 2 mm. Full details on the microplasma process can be found in our previous work [17, 18]. The process was repeated 4 times and after ethanol evaporation about 10 mg powder was produced. The powder of microplasma-processed Si-ncs (7.5 mg) was mixed with an aqueous solution of PEDOT:PSS (3 mL) and then spin-coated to form a Si-ncs/PEDOT:PSS nanocomposite film with a thickness

Nanoscale Accepted Manuscript

of about 100 nm onto an indium-tin-oxide-coated glass substrate. In order to limit the deterioration of the absorption of the PTB7 based solar cell the concentration of Si-ncs in PEDOT:PSS nanocomposite film for fabrication of solar cells was selected to do not reduce significantly light transmittance in the 450 -700 nm range. After spin-coating, the deposited layer was dried at 135 °C for 10 min in air. For reference and comparison, we repeated the same procedure for a PEDOT:PSS layer without Si-ncs.

Device fabrication - After depositing the nanocomposite (with Si-ncs) or the PEDOT:PSS layer only (without the Si-ncs), the devices were completed with a 100 nm thick organic active layer and metal contacts. The active layer was fabricated by spin coating PTB7: [70]PCBM (8 mg and 12 mg, respectively), dispersed in 1 mL chlorobenzene; we also added 3% of diiode octane as additive in the PTB7:[70]PCBM solution and dried at room temperature in a glove box filled with nitrogen. In the case of hybrid solar cells 25 wt% of surface-engineered Si-ncs was added to the PTB7:[70]PCBM blend in the glove box. It has to be noted that in this case Si-ncs would not need to undergo surface engineering by microplasma, because Si-ncs disperse easily in chlorobenzene. However, the surface engineering process enhances the interaction of Si-ncs with PTB7 and also the photovoltaic properties [19]. Also, the morphology of Si-ncs in PTB7 was previously studied and it was observed that at these concentrations, the presence of the Si-ncs did not introduce major morphology changes [19]. Finally, a lithium fluoride layer (0.1 nm thick) and the aluminum electrodes (100 nm thick) were deposited by vacuum evaporation. The active area of each cell was 4 mm^2. The J-V and EQE characteristics of the solar cells were evaluated at room temperature in N_2 atmosphere. In all cases, the irradiance was calibrated by a standard a-Si solar cell.

Nanoscale Accepted Manuscript

3. Results and Discussion

Our general device structure include a glass substrate with an indium-tin-oxide coating, a PEDOT:PSS layer (with or without Si-ncs), the active layer formed by a polythieno[3,4-b]thiophenebenzodithiophene (PTB7):[6,6]-phenyl-C71-butyric acid ([70]PCBM) bulk heterojunction (with or without Si-ncs), an LiF layer and finally Al electrodes. We also analyze the beneficial contribution of the Si-ncs with increasing light intensity; as a way of understanding the effect of increasing light intensity, we evaluate solar cell devices under low-concentrated light (1-sun, 2-suns and 4-suns).

When Si-ncs are included in the PEDOT:PSS layer only, the nanocrystals are optically active but do not contribute to carrier dissociation and transport. Because the active layer is formed by polymers only, this type of device is essentially an organic bulk-heterojunction. The inclusion of Si-ncs in PEDOT:PSS is a suitable choice for PV applications because PEDOT:PSS is one of the most promising conducting polymers being used in PVs due to its high conductivity, high transmittance in the visible range, excellent stability, water solubility and very good film-forming properties [1]. PEDOT:PSS is often used in device architectures to facilitate the fabrication of polymer solar cells and it is deposited before the organic active layer. The use of Si-ncs as optical converters requires the Si-ncs to be integrated and deposited before the active layer, therefore the fabrication of a conductive inorganic/organic hybrid nanocomposite made of Si-ncs embedded in the PEDOT:PSS matrix would be a desirable approach. However, after synthesis, Si-ncs are highly hydrophobic and do not easily disperse in aqueous solutions [17] with consequent difficulties in producing a water-based Si-ncs/PEDOT:PSS colloid as required

Nanoscale Accepted Manuscript

for the deposition of the hybrid nanocomposite film. Furthermore, Si-ncs in contact with water are prone to uncontrolled and inward oxidation that leads to the degradation of the optical properties [17]. In order to improve the dispersion of Si-ncs in water, ultrasonication has been previously used; however, ultrasonication has negative effects on the fine structure of the PEDOT:PSS network and results in the deterioration of the carrier mobility of the film [24]. Also, ultrasonication has shown to accelerate the Si-ncs inward oxidation process [25].

In order to modify the hydrophobic character, to allow water dispersion and to prevent the uncontrolled inward oxidation of the Si-ncs, we have developed a surface engineering process based on an atmospheric-pressure microplasma treatment [18, 26]. The microplasma treatment is carried out on a colloid of Si-ncs in ethanol; following, the Si-ncs are dried and re-dispersed in an aqueous solution of PEDOT:PSS. This procedure yields highly photoluminescent and water-stable Si-ncs at room temperature with hydrophilic surface characteristics and without using large organic molecules or other surfactants. These characteristics are achieved thanks to the formation of molecular bonds of the type Si-O-R at the surface of the Si-ncs [18]; full details on the optical properties of these surface-engineered Si-ncs can be found in our previous work [17, 18, 27] and in the Supporting Material. The Si-ncs/PEDOT:PSS colloid is then spin-coated to form the nanocomposite film after annealing at 135 °C. The heat treatment is generally applied to PEDOT:PSS films to establish high conductivity and high transmittance [28] and we have verified that 135 °C have no effect on the PL properties of the Si-ncs embedded in PEDOT:PSS. Figure 1a shows typical PL spectra for Si-ncs after microplasma processing in ethanol (blue line) and Si-ncs/PEDOT:PSS composite film before (symbols) and after annealing at 135 °C (red line). It should be noted that the PL intensity of the surface-engineered Si-ncs in ethanol (multiplied by 0.01) is not directly comparable with the PL of the nanocomposite as the first is measured for the

Nanoscale Accepted Manuscript

colloid and therefore the concentration of the Si-ncs is different compared to the Si-ncs concentration in the film. A small blue shift is observed comparing the surface-engineered Si-ncs in colloid and PL peak wavelength of the nanocomposites. This is due to a limited degree of oxidation during the fabrication of the nanocomposite. In figure 1a we also report the PL of the PEDOT:PSS film without Si-ncs (black line) which does not exhibit any PL at room temperature in the visible spectral region and confirms that the PL in the nanocomposite originates from the Si-ncs. The PL maximum (at ~590 nm) of the nanocomposite after annealing at 135 °C is unchanged (red line). This supports the effectiveness of the surface chemistry, which may have prevented degradation of the Si-ncs even after annealing in air. A slight increase in the PL intensity is most likely due to the densification of the PEDOT:PSS polymer and an improved passivated interface between the Si-ncs and polymer. Fig 1b shows corresponding absorption spectra of the Si-ncs/PEDOT:PSS composites after annealing at 135 °C (red line) and Si-ncs only (black line).

Nanoscale Accepted Manuscript

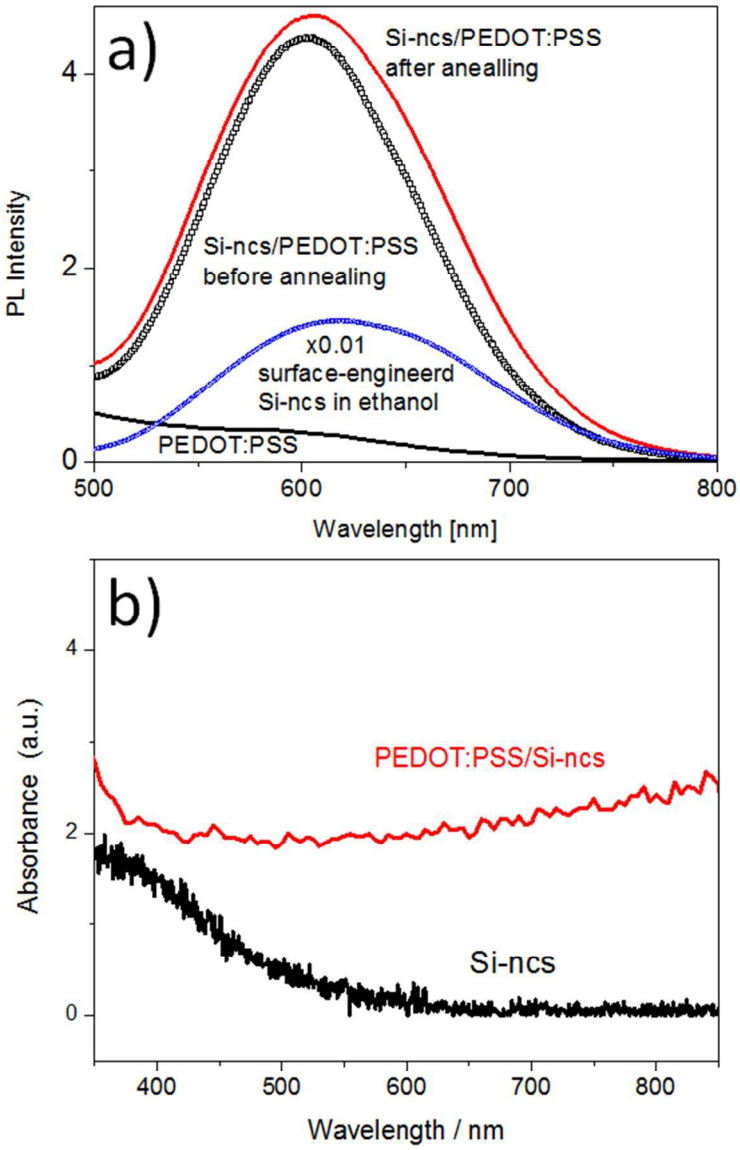

Figure 1. a) Photoluminescence (PL) spectra for silicon nanocrystals (Si-ncs) after microplasma processing in ethanol (blue small squares) and Si-ncs/PEDOT:PSS composites before (black large squares) and after annealing at 135 °C (red line). The PL of the PEDOT:PSS film without Si-ncs after annealing at 135 °C is shown for comparison (black line). b) Absorption spectra of the Si-ncs/PEDOT:PSS composites after annealing at 135 °C (red line) and of the Si-ncs only (black line).

Nanoscale Accepted Manuscript

The Si-ncs/PEDOT:PSS nanocomposite is then used in organic solar cell devices. We have compared the performance of PTB7:[70]PCBM solar cells that used a PEDOT:PSS layer without Si-ncs with the performance of PTB7:[70]PCBM devices that used our new Si-ncs/PEDOT-PSS nanocomposite (figure 2a). Here we expect the Si-ncs to absorb UV-photons and prevent their penetration in the PTB7:[70]PCBM active layer converting them into lower-wavelength photons. Figure 2b shows typical current density versus voltage (J-V) characteristics under 100 mW cm^{-2} irradiance (1 sun). The device with the Si-ncs/PEDOT-PSS nanocomposite exhibited a slight improvement in the fill factor (*FF*) from 68% to 71% and maintained the same open-circuit voltage (V_{OC}) at 0.76 V. The short-circuit current density (J_{SC}) was reduced from 14.26 mA cm^{-2} to 13.69 mA cm^{-2} representing a small change also reflected in negligible variations in the power conversion efficiency from 7.41% to 7.33%. The decrease in photocurrent generation may be in part due to a diminished carrier mobility in the PEDOT:PSS layer due to the presence of the Si-ncs. However, it is also likely that the presence of the Si-ncs is reducing light transmittance to the active layer in the 450-700 nm range; this is supported by the decrease of the external quantum efficiency (EQE) in the region from 450 nm to 700 nm (figure 2c). Nevertheless in the region where Si-ncs absorption and down-conversion occur (below ~400 nm) the EQE curve of the device with the nanocomposite (black line in figure 2c) is higher than the EQE of the device with PEDOT:PSS only (red line in figure 2c).

Nanoscale Accepted Manuscript

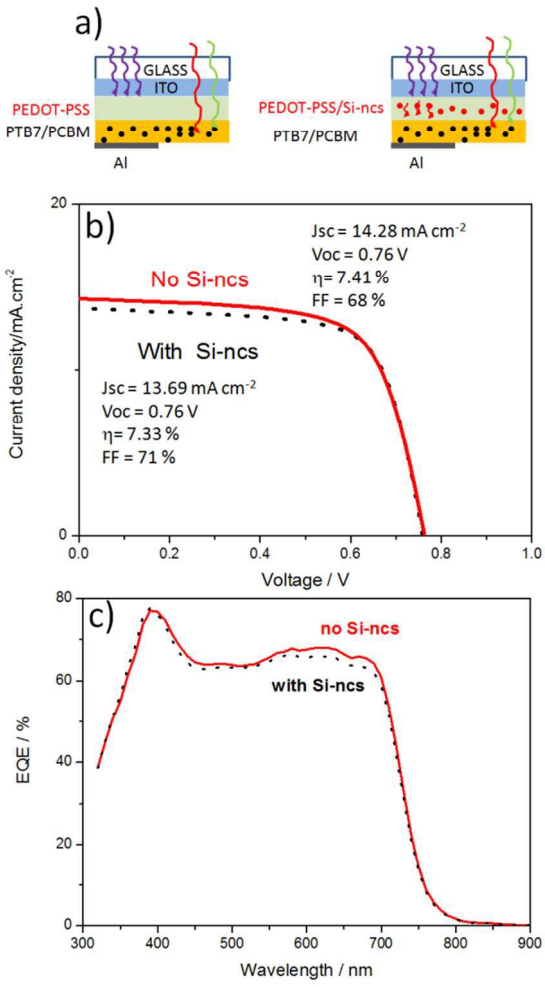

Figure 2. a) Schematic device structure without (left) and with (right) silicon nanocrystals (Si-ncs) in the PEDOT:PSS layer. b) Current density versus voltage characteristics and c) corresponding external quantum efficiency (EQE) of solar cells with (black dotted line) and without (red full line) Si-ncs in the PEDOT:PSS layer under 1 sun irradiance.

Because a higher photon flux is expected to increase the Si-ncs PL intensity [25], we would also expect an enhancement of the Si-ncs contribution with concentrated sunlight radiation. Therefore, figure 3a compares the J-V characteristics with 100 mW cm^{-2} (1 sun), 200 mW cm^{-2} (2 suns) and 400 mW cm^{-2} (4 suns) irradiance for solar cell without (full lines) and

Nanoscale Accepted Manuscript

with the Si-ncs (dotted lines). The device performance parameters are also summarized in Table 1.

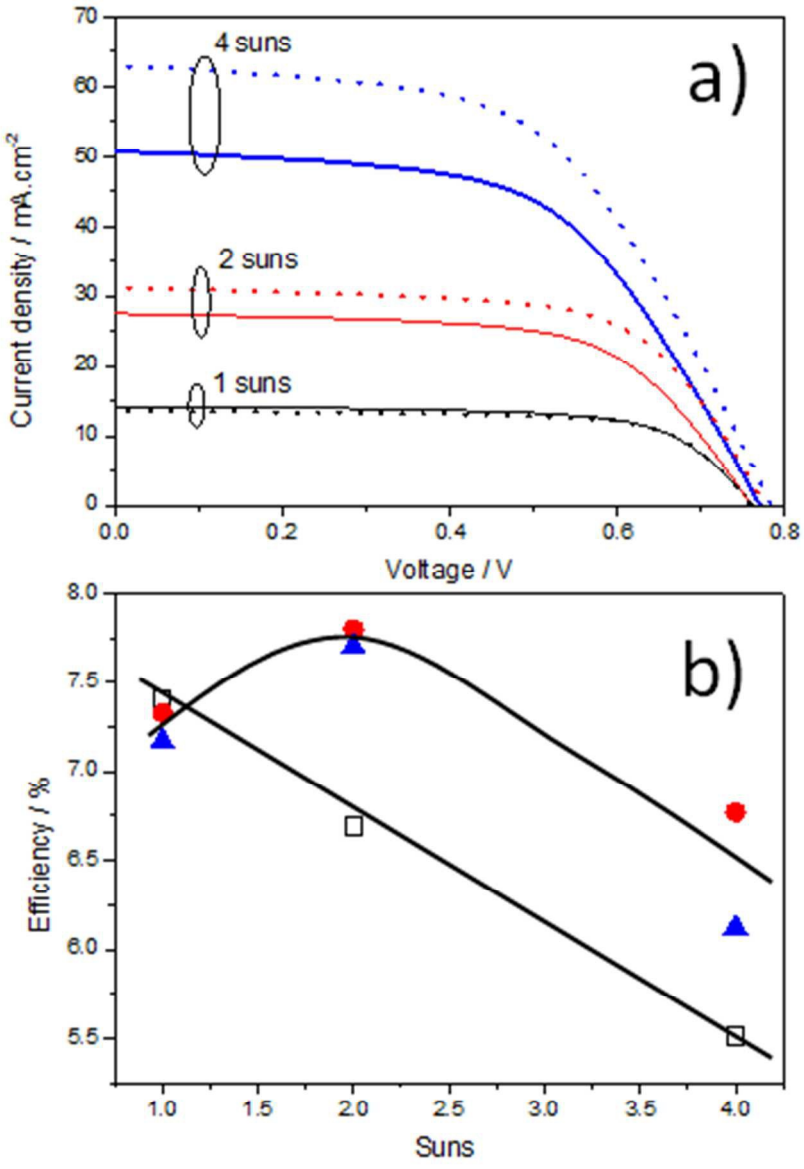

Figure 3. a) Current density versus voltage (J-V) curves of PTB7:[70]PCBM solar cells with (full lines) and without (dotted lines) Si-ncs in the PEDOT:PSS layer under irradiation at different levels of concentrated light; b) conversion efficiencies of solar cell devices without

Nanoscale Accepted Manuscript

(open symbols) and with Si-ncs (full symbols); full red circles and full blue triangles refer to repeated devices.

	Organic Solar Cell Devices							
	without Si-ncs				with Si-ncs			
Suns	**V_{OC} (V)**	**I_{SC} (mA cm^{-2})**	**FF (%)**	**Efficiency (%)**	**V_{OC} (V)**	**I_{SC} (mA cm^{-2})**	**FF (%)**	**Efficiency (%)**
1-sun	0.76	14.28	68	7.41	0.76	13.69	71	7.33
2-suns	0.77	27.57	63	6.69	0.78	31.13	65	7.80
4-suns	0.77	50.69	56	5.51	0.78	62.92	55	6.77

Table 1. Representative performance parameters for devices with and without silicon nanocrystals at three different levels of concentrated light (suns).

The V_{OC} remains essentially constant (less than 3% variation in all cases) as a function of irradiance. The two types of devices are also consistent in exhibiting a decreasing *FF* with increasing concentration (table 1); because the open-circuit voltage is essentially invariant, increased carriers recombination at the PTB7:[70]PCBM interface cannot be responsible for reducing the *FF* [29]. Most likely, the voltage across the series resistance increases due to higher current densities under concentrated sunlight and consequently affect negatively the *FF*. Importantly, considerable and clear difference between the two types of devices, i.e. with and without Si-ncs, is observed for the J_{SC} under increased irradiance. The 1-sun short-circuit current is slightly lower (by ~4%) for the solar cell with the nanocomposite (13.69 mA cm^{-2}) compared to the 1-sun J_{SC} of the device without Si-ncs (14.28 mA cm^{-2}). However, with concentrated light, the devices with Si-ncs exhibit much larger short-circuit current densities with respect to devices without Si-ncs: 31.13 mA cm^{-2} vs. 27.57 mA cm^{-2} at 2-suns (~13% increment) and 62.92 mA cm^{-2} vs. 50.69 mA cm^{-2} at 4-suns (~24% increment). In both types of devices, J_{SC} increases linearly with the irradiance, however a much steeper gradient is observed for the cell with the Si-ncs/PEDOT:PSS nanocomposite. The linear behavior is expected because the number of carriers is directly proportional to the number of photons absorbed.

Nanoscale Accepted Manuscript

Figure 3b summaries the conversion efficiency of solar cells without (open symbols) and with (full symbols) the Si-ncs in the PEDOT:PSS layer. The device without the Si-ncs showed a linear decreasing trend as the sunlight concentration was increased (figure 3b, open symbols); on the contrary, the solar cells with the Si-ncs/PEDOT-PSS nanocomposite exhibited a non-linear behavior with a maximum efficiency at about 2-suns (figure 3b, full symbols) for the results reported here and with an overall better performance under concentrated light; it is clear that the actual maximum efficiency may have occurred anywhere between 1-sun and 4-suns.

Organic devices under concentrated light are anticipated to exhibit higher current densities because the number of charged carriers generated is directly proportional to the number of photons absorbed. However, with concentrated light, the overall efficiency of organic devices is expected to decrease because intense light is detrimental to polymers transport properties. The devices without the Si-ncs nanocomposite are therefore behaving as expected, i.e. the J_{SC} increases linearly with solar concentration and the device efficiency decreases linearly. The non-linear behavior of the devices with the nanocomposite is evidence of a mechanism that is contributing to increasing the device efficiency for > 1-sun concentration and is eventually superseded by the degrading polymer transport properties at 4-suns. We suggest that this mechanism can be identified with the down-conversion of the Si-ncs which essentially increases the lower wavelength photon flux to the active layer and increases the current density of the devices with Si-ncs (see figure 3a).

We will now discuss also the effect of the down-converting nanocomposite in hybrid solar cell devices. Hybrid devices are produced by introducing 25 wt.% Si-ncs also in the active layer of the PTB7:[70]PCBM bulk-heterojunction. The device is in this case referred to as a

Nanoscale Accepted Manuscript

hybrid organic/inorganic bulk-heterojunction because it includes an electronically active inorganic component (i.e. the Si-ncs). Therefore, in this case, we expect the Si-ncs to affect also the dissociation efficiency and transport properties of the device. It has been shown that the Si-ncs within conjugated polymers can act as acceptors with decent device efficiencies [5, 19]; however the Si-ncs performance is still relatively poor, possibly due to a lower capacity for the Si-ncs to accept the electrons in comparison to [70]PCBM.

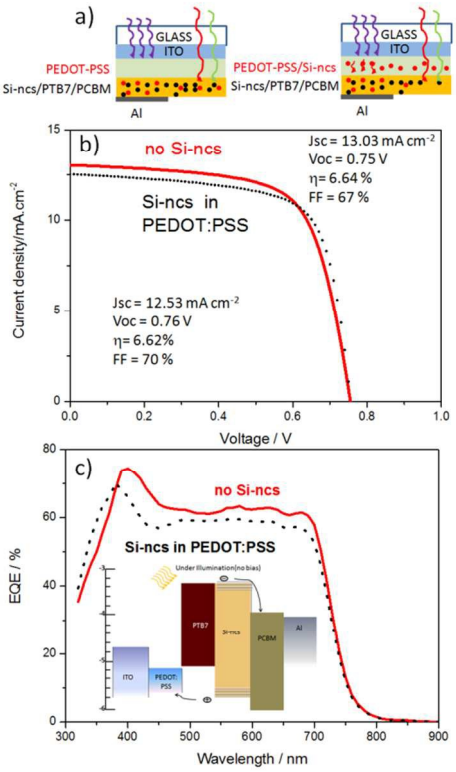

Figure 4. a) Schematic structure of hybrid devices without (left) and with (right) silicon nanocrystals (Si-ncs) in the PEDOT:PSS layer. b) Current density versus voltage (J-V) curves of solar cells without and with the Si-ncs/PEDOT:PSS nanocomposite under 1-sun irradiation. c)

Nanoscale Accepted Manuscript

Corresponding external quantum efficiencies of the device without and with Si-ncs in PEDOT:PSS layer; the inset shows the energy band diagram of the device architecture.

Figure 4a shows the schematic structures of the devices without and with Si-ncs in the PEDOT:PSS layer; both hybrid devices of figure 4a include Si-ncs in the active layer, therefore, hereafter, we will use "with/without Si-ncs" only to refer to the presence of the Si-ncs in the PEDOT:PSS down-conversion layer. Figure 4b compares the J-V characteristic of hybrid solar cells without and with Si-ncs in the PEDOT:PSS layer under 1-sun irradiation and figure 4c reports on the corresponding EQE characteristics. The inset of figure 4c shows the energy band diagram of the device.

The performance of the solar cell with the Si-ncs introduces identical effects in the hybrid device architecture as they were observed for fully-organic devices (compare figure 4b with 2b and 4c with 2c). The Si-ncs in the PEDOT:PSS layer do not visibly influence the overall conversion efficiency (~6.6%) in hybrid devices (figure 4b), exhibiting a slight improvement in the *FF*, maintaining about the same V_{OC} and reducing slightly the short-circuit current density. Similarly to the organic devices (figure 2), the decrease in photocurrent may be due to a diminished carrier mobility in the PEDOT:PSS layer and due to the reduced light transmittance to the active layer in the 450-700 nm range; the latter is also in this case supported by the decrease of the EQE in the region from 450 nm to 700 nm (figure 4c). Furthermore, the increased EQE in the region where the Si-ncs absorption and down-conversion is expected to occur (below ~410 nm) is also confirmed; see blue line in figure 4c for the devices with the Si-ncs vs. the red line for the devices without the Si-ncs.

Nanoscale Accepted Manuscript

Furthermore, the same trends are observed when hybrid devices with/without Si-ncs in the PEDOT:PSS layer are studied under concentrated light. Figure 5a presents current density versus voltage curves of hybrid solar cells with (dotted lines) or without (full lines) the Si-ncs in the PEDOT:PSS layer under 100 mW/cm^2, 200 mW/cm^2 and 400 mW/cm^2 irradiance. Figure 5 can be directly compared with figure 3, which reports on corresponding devices with a fully organic active layer. The device performance parameters of figure 5 are also summarized in Table 2.

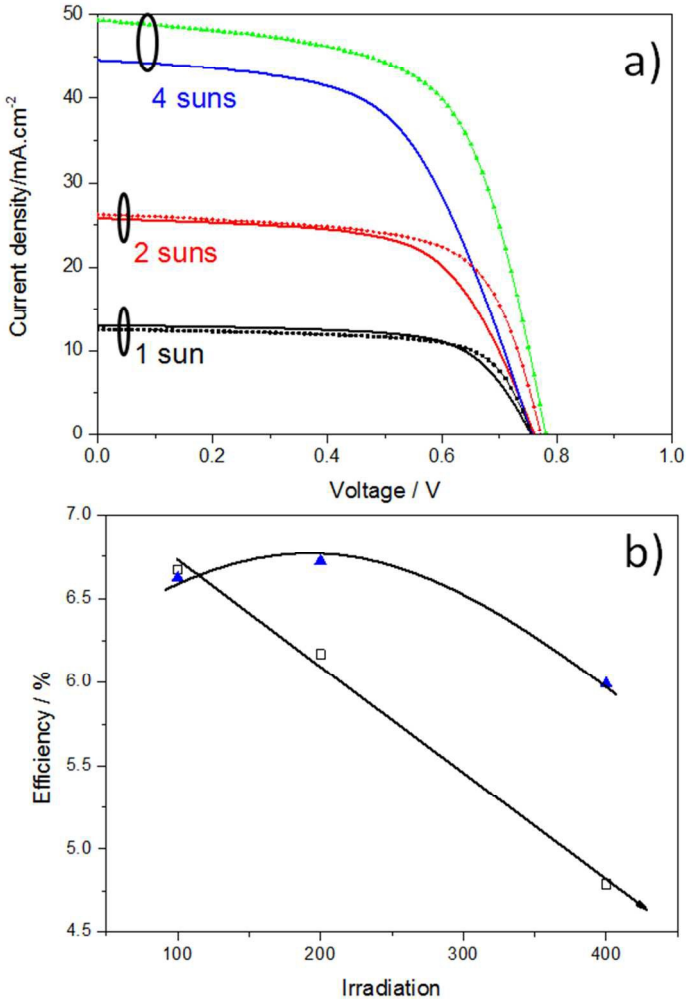

Nanoscale Accepted Manuscript

Figure 5. a) Current density versus voltage curves of solar cells with 25 wt.% silicon nanocrystals (Si-ncs) in the PTB7:[70]PCBM active layer with (dotted lines) and without (full lines) the Si-ncs in the PEDOT:PSS layer under 1-, 2-, and 4-suns irradiation. b) Corresponding conversion efficiency of devices without (open symbols) and with Si-ncs (full symbols) in PEDOT:PSS layer.

	Hybrid Solar Cell Devices							
	without Si-ncs				with Si-ncs			
Suns	**V_{OC} (V)**	**I_{SC} (mA cm^{-2})**	**FF (%)**	**Efficiency (%)**	**V_{OC} (V)**	**I_{SC} (mA cm^{-2})**	**FF (%)**	**Efficiency (%)**
1-sun	0.75	13.03	67	6.64	0.76	12.53	70	6.62
2-suns	0.76	25.76	63	6.17	0.77	26.21	66	6.72
4-suns	0.76	44.61	57	4.79	0.78	49.36	62	5.99

Table 2. Performance parameters for devices with and without silicon nanocrystals at three different levels of concentrated light (suns).

Under concentrated light, in all cases, the introduction of Si-ncs in the PEDOT:PSS layer (dotted lines in both figure 3 and figure 5) is beneficial to the overall performance of the solar cell. Since under concentrated light Si-ncs clearly show nonlinear PL properties [30], it is reasonable and highly likely that the device improvements originate from the down-conversion of high energy photons into red-photons [11, 31]. The nanocomposite also slightly improves the V_{OC} to 0.78 V in both organic and hybrid devices and the efficiency non-linear behavior of organic devices (Figure 3b) due to the Si-ncs/PEDOT:PSS layer is again observed for hybrid solar cells (Figure 5b). In summary, the results from 15 devices are reported here for the same Si-ncs/PEDOT:PSS nanocomposite material providing a consistent picture of its performance. These results also strongly support the repeatability and reliability of the Si-ncs/PEDOT:PSS nanocomposite layer under different conditions and within a range of different devices.

Nanoscale Accepted Manuscript

The effectiveness of the down-conversion result from the balance between absorption of the Si-ncs at the lower wavelengths and the quantum yield (QY) of the Si-ncs that determine the re-emission at a more favorable wavelength range. The contribution of the down-conversion mechanism can be inferred from the QY of the Si-ncs. The initial QY of our Si-ncs is ~10%, which can be increased to ~30% with surface engineering by microplasma (see Supporting Material); we can therefore assume that the efficiency of down-conversion could be readily obtained by this figure considering the isotropic nature of the PL. Also, it has to be noticed that the initial 10% is relatively modest and that QY above 80% could be achieved using optimized Si-ncs produced for instance by plasmas [32, 33]. Therefore it is clear that the down conversion effect and efficiency improvement could be dramatically higher and in particular efficiency improvements could be achieved even at 1-sun, without concentration.Since down conversion can be in principle tuned by Si-ncs size and the concentration, another advantage of embedding Si-ncs/PEDOT:PSS nanocomposites could be the integration with tandem solar cells whereby easier matching of photocurrents of top with bottom cell can be more easily achieved [34].

Although the effect of the Si-ncs in the active layer is not the main focus of this work, it may be important to highlight some important aspects of the Si-ncs direct contribution to carrier generation and transport. This can be done by comparing the results that relate to the devices without the Si-ncs in the down-conversion PEDOT:PSS layer, i.e. the red curves of figure 2b-c with the red curves of figure 4b-c and the corresponding performance parameters (i.e. the greyed rows in table 1 and table 2). The V_{OC} and *FF* are not affected by the introduction of Si-ncs in the active layer, however the current density is visibly reduced, which is the main cause of lower

Nanoscale Accepted Manuscript

efficiencies for devices with the Si-ncs in the active layer. A range of factors may have contributed to decrease the device performance. The Si-ncs necessarily prevents the organic interface to function as in standard organic solar cells, degrading its performance due to both a reduced absorption (note that polymer absorption is ~10 higher than Si-ncs) as well as a compromised organic junction. At the same time, at the conditions of figure 4-5, the benefits of the Si-ncs layer may be still limited so that overall, the device with the Si-ncs has suffered in terms of performance. The unaffected V_{OC} and *FF* support this argument and may suggest that an optimized concentration of the Si-ncs in the active layer may lead to a beneficial contribution of the Si-ncs. More specifically, the *FF* confirms that the architecture with Si-ncs in the active layer is not morphologically affected. Furthermore, the V_{OC} behavior in figure 5b suggests that the Si-ncs in the active layer are not negatively affecting dissociation efficiency and in light of the reduced absorption may instead contribute to it. It is possible that Si-ncs higher density of states provides dissociation sites for exciton created in the polymer hetero-junction and/or contribute to change favorably the alignment between energy levels. The Si-ncs concentration needs therefore to be optimized to preserve these beneficial effects vs. the reduced absorption. Finally, it may be important to highlight that the presence of the Si-ncs in the active layer may have enhanced the down-conversion mechanism. This can be observed by comparing figure 2c and figure 4c in the range below 410 nm. The enhancement of the EQE due to Si-ncs in the PEDOT:PSS layer is much more pronounced when the Si-ncs are also in the active layer (see the "*Si-ncs in PEDOT:PSS*" blue line vs. the "*no Si-ncs*" red line, in figure 4c) compared to the fully-organic devices without Si-ncs in the active layer (see the "*with Si-ncs*" black line vs. the "*no Si-ncs*" red line, in figure 2c).

Nanoscale Accepted Manuscript

4. Conclusions

We have demonstrated the possibility of easily introducing Si-ncs in organic device architectures with different contributions to the solar cell performance. Surface-engineered Si-ncs by microplasma offer excellent opportunities for optimized interactions with polymers derived from easily processed colloids in water and other solvents (e.g. chlorobenzene). The Si-ncs water-based nanocomposite has resulted in an important contribution in the device efficiency when used as an optical down-converter with enhanced photocurrent generation. With concentrated light (< 10-suns), the use of photoluminescent surface-engineered Si-ncs introduces advantages to organic and hybrid devices whereby both efficiency and durability can be improved. Importantly, it is also confirmed that the nanocomposite-induced down-conversion performs better at increased but still relatively low light intensity (< 2-suns), which represents an important range of radiation intensity largely determined by geographical location and weather conditions. When Si-ncs were integrated in the active layer the overall device performance suffered from reduced absorption. However, the V_{OC} and *FF* are in support of a positive contribution and most importantly, the presence of the Si-ncs in the active layer enhances the down-conversion effect of Si-ncs. Therefore, tuning the concentration of Si-ncs in both the PEDOT:PSS as well as in the active layer, represent an opportunity to increase/decrease the EQE in different part of the spectrum and tailor the conversion efficiency.

Nanoscale Accepted Manuscript

Acknowledgement

This work was partially supported by a NEDO project, the Royal Society International Exchange Scheme (IE120884), the Leverhulme International Network (IN-2012-136) and EPSRC (EP/K022237/1). DM also acknowledges the support of the JSPS Bridge Fellowship and SM thanks the financial support of the University of Ulster Vice-Chancellor Studentship.

Nanoscale Accepted Manuscript

REFERENCES

1. Pi, X. D.; Liptak, R. W.; Deneen Nowak, J.; Wells, N. P.; Carter, C. B.; Campbell, S. A.; Kortshagen, U. Air-Stable Full- Visible-Spectrum Emission from Silicon Nanocrystals Synthesized by an All-Gas-Phase Plasma Approach. *Nanotechnology* **2008**, 19, 245603-245609.

2. Pavesi, L.; Dal Negro, L.; Mazzoleni, C.; Franzò, G ; Priolo, F. Optical gain in silicon nanocrystals. *Nature* **2000**, 408, 440-444.

3. Kovalev, D.; Fujii, M. Silicon Nanocrystals: Photosensitizers for Oxygen Molecules. *Adv. Mater.* **2005**.17, 2531-2544.

4. Timmerman, D.; Izeddin, I. ; Stallinga, P. ; Yassevich, I. N.; Gregorkiewicz, T. Space-separated quantum cutting with Si nanocrystals for photovoltaic applications. *Nat. Photonics* **2008**, 2, 105-109.

5. Liu, C.-Y.; Holman, Z. C. ; Kortshagen, U. R. Optimization of Si NC/P3HT Hybrid Solar Cells. *Adv. Funct. Mater*. **2010**, 20, 2157-2164.

6. Hua, F.; Swihart, M. T.; Ruckenstein, E. Efficient Surface Grafting of Luminescent Silicon Quantum Dots by Photoinitiated Hydrosilylation. *Langmuir* **2005**, 21, 6054–6062.

7. Nozik, A. J. Nanoscience and Nanostructures for Photovoltaics and Solar Fuels. *Nano Lett.* **2010**, 10, 2735- 2742.

Nanoscale Accepted Manuscript

8. Sark V. ; Meijerink M.; Schropp, R.E.I.; Van Roosmalen, J.A.M.; Lysen, E.H.; Enhancing solar cell efficiency by using spectral converters, *Solar Energy Materials & Solar Cells*. **2005** 87, 395-409.

9. Grossiord N.; Kroon J.M.; Andriessen R.; Blom P. W.M.; Degradation mechanisms in organic photovoltaic devices, *Organic Electronics* **2012** 13 432–456.

10. Sgrignuoli F.; Ingenhoven P.; Pucker G.; Mihailetchi V.D.; Froner E.; Jestin Y.; Moser E.; Sànchez G.; Pavesi L. Purcell effect and luminescent downshifting in silicon nanocrystals coated back-contact solar cells*, Solar Energy Materials & Solar Cells*, **2015** 132, 267–274.

11. Švrcek V.; Slaoui A.; and Muller, J.-C. Silicon nanocrystals as light converter for solar cells, *Thin Solid Films* **2004**, 451, 384-391.

12. Švrcek V.; Yamanari T.; Mariotti D.; Mitra, S.; Matsubara K.; Kondo M., Enhancement of Polymer Solar Cell Performance under Low-Concentrated Sunlight by 3D Surface-engineered Silicon Nanocrystals, 39th IEEE Photovoltaic Specialists Conference, Tampa Florida, June **2013**, Proc. on CD A1-911 (1-5) *, A0-911, 1-5*

13. Cotal H.: Fetzer Ch.; Boisvert J.; Kinsey G.; King R.; Hebert P.; Yoon H.; Karam N.; III–V multijunction solar cells for concentrating photovoltaics, *Energy Environ. Sci.*, **2009**, 2, 174–192.

14. Yao E.P.; Ho C.S.; Yu C.; Huang E. L.; Lai Y. N.; and An W. C.H.; Alternative Approach for Improving Performance of Organic Photovoltaics by Light-Enhanced Annealing, *International Journal of Photoenergy,* **2014** , Article ID 120693

Nanoscale Accepted Manuscript

15. Batchelder J. S. ; Zewail A. H.; Cole T. Luminescent solar concentrators. Experimental and theoretical analysis of their possible efficiencies, *Appl. Opt.* **1981**, 20, 3733-3740.

16. Currie M. J; Jonathan K. Mapel, J.K.; Heidel T.D.; Goffri S.; Baldo M.A.: High-Efficiency Organic Solar Concentrators for Photovoltaics, *Science* **2008**, 321, 226-230.

17. Mariotti, D.; Mitra. S.; Švrcek, V.; Surface-engineered silicon nanocrystals, *Nanoscale* **2013**, 5 (4), 1385 – 1398.

18. Švrcek, V.; Mariotti, D.; Kondo. M._ Microplasma-induced surface engineering of silicon nanocrystals in colloidal dispersion. *Appl. Phys. Lett.* **2010**, 97, 161502(1-3).20.

19. Švrcek V.; Yamanari T.: Mariotti D.; Matsubara K.; Kondo M.; Enhancement of hybrid solar cell performance by polythieno [3,4-b]thiophenebenzodithiophene and microplasma-induced surface engineering of silicon nanocrystals, *Appl. Phys. Lett.* **2012** 100, 223904(1)-223904 (4)

20. Mitra S.; Švrček V.; Mariotti D.; Matsubara K.; Kondo M.; Microplasma-induced liquid chemistry as a tool for stabilization of silicon nanocrystals optical properties in water, *Plasma Processes and Polymers* **2014**, 11**,** 158-163.

21. Pavesi, L.; Turan, R., *Silicon nanocrystals: fundamentals, synthesis and applications*.Wiley-VCH Verlag GmbH & Co. KGaA, **2010**.

22. Wolkin, M.; Jorne, J.; Fauchet, P.; Allan, G.; Delerue, C. Electronic States and Luminescence in Porous Silicon Quantum Dots: The Role of Oxygen. *Phys. Rev. Lett.* **1999**, *82*, 197-200.

Nanoscale Accepted Manuscript

23. Ogata, Y. H.; Yoshimi, N. ; Yasuda, R. ; Tsuboi, T. ; Sakka, T. ; Otsuki, A. Structural Change in P-type Porous Silicon by Thermal Annealing. *J. Appl. Phys.* **2001**, *90*, 6487-*6492.*

24. Kim H.; Lee J.; Ok S.: Choe Y.; Effects of pentacene-doped PEDOT:PSS as a hole-conducting layer on the performance characteristics of polymer photovoltaic cells, *Nanoscale Res Lett.* **2012**; 7(1): 5-11.

25. Liu, Y. ; Chen, T. P.; Ng, C. Y. ; Ding, L. ; Zhang, S. Fu, Y. Q. ; Fung, S. Depth profiling of charging effect of Si nanocrystals embedded in SiO2: a study of charge diffusion among Si nanocrystals. *J. Phys. Chem. B* **2006**, 110, 16499-16502

26. Mitra S.; Cook S.; Švrček V.; Blackley R. A.; Wuzong Z.; Kovač J.; Cvelbar U.; Mariotti D.; Improved optoelectronic properties of silicon nanocrystals/polymer nanocomposites by microplasma-induced liquid chemistry, *Journal of Physical Chemistry C* **2013**, 117, 23198-23202.

27. Svrcek V.; Dohnalova K.; Mariotti D.; Trinh M. T.; Limpens R.; Mitra S.; Gregorkiewicz T,; Matsubara K.; and Kondo M.; Dramatic Enhancement of Photoluminescence Quantum Yields for Surface-Engineered Si Nanocrystals within the Solar Spectrum, *Adv. Funct. Mater.* **2013**, 23, 6051-6058.

28. Alemu D.; Wei H-Y.; Ho K-Ch.; Chu Ch-W.; Highly conductive PEDOT:PSS electrode by simple film treatment withmethanol for ITO-free polymer solar cells *Energy Environ. Sci.,* **2012**, 5, 662-669.

Nanoscale Accepted Manuscript

29. Kemp K.W.; Labelle A.J.; Thon S.M.; Ip A.H.; Kramer I.J.; Hoogland S.; Sargent E.H.; Interface Recombination in Depleted Heterojunction, Photovoltaics based on Colloidal Quantum Dots, *Adv. Energy Mater.* **2013**, **3**, 917–921.

30. Luterová K. ; Dohnalová K.; Švrcek V.; Pelant I.; Likforman J. P.; Cregut O.; Gilliot P. ; Honerlage B.; Optical gain in porous silicon grains embedded in sol-gel derived SiO_2 matrix under femtosecond excitation, *Appl. Phys. Lett.* **2004**, 84, 3280.

31. Huang C. Y.; Wang D. Y.; Wang C. H.; Chen Y. T.; Wang Y. T.; Jiang Y. T.; Yang Y. J. ; Chen C. C.; and Chen Y. F.; Efficient Light Harvesting by Photon Downconversion and Light Trapping in Hybrid ZnS Nanoparticles/Si Nanotips Solar Cells, *ACS Nano*, **2010**, 4 (10), pp 5849–5854.

32. Miller J.B; Van Sickle A.R; Anthony R.j.; Kroll, D.M; Kortshagen U.R;; Hobbie E.K.; Ensemble brightening and enhanced quantum yield in size-purified silicon nanocrystals**,** *ACS Nano*. **2012**; 6(8):7389 -7396.

33. Askari, S. ; Levchenko, I. ; Ostrikov K.; Maguire P.; and. Mariotti D.; Crystalline Si nanoparticles below crystallization threshold: Effects of collisional heating in non-thermal atmospheric-pressure microplasmas; *Appl. Phys. Lett.* **2014**, 104, 163103.

34. Kerestes C.; Wang Y.; Shreve K.; Mutitu J.; Creazzo T. ; Murcia P.; Barnett A. Design, fabrication, and analysis of transparent silicon solar cells for multi-junction assemblies, *Prog. Photovoltaics: Res. Appl.* **2013**, 21, 578–587.

Nanoscale Accepted Manuscript